TECHNICAL UNIVERSITY OF LODZ

FACULTY OF MECHANICAL ENGINEERING

Division of Dynamics

Michał Marszal
137883

MASTER OF SCIENCE THESIS
Mechanical Engineering and Applied Computer Science
Full-time studies

DYNAMICS OF DOUBLE PENDULUM WITH PARAMETRIC HORIZONTAL EXCITATION

supervisor:
prof. dr hab. inż. Tomasz Kapitaniak

INNOVATIVE ECONOMY
NATIONAL COHESION STRATE
FNP
Foundation for Polish Science
EUROPEAN UNION
UROPEAN REGIONAL
EVELOPMENT FUND

ŁÓDŹ 11.07.2011

Contents

Chapter 1

Introduction

Pendulum is a classic mechanical device used by human beings for ages. Among scientists who investigated pendulum's properties were famous names such as Galileo, Huygens, Newton, Hooke. Using pendulum, fundamental laws of classic mechanics were determined (collisions law, conservation law, value of gravitational acceleration). The variation of gravitation acceleration due to shape of the earth were proved, not to mention the Foucault pendulum giving evidence to rotation of the earth. The pendulum contributed to revolution in horology, when Huygens's pendulum clock was more accurate than mechanical clocks of that time.

The simple pendulum when subjected to small angular displacement oscillates with the natural frequency dependent only on its length. It represents simple harmonic motion. One has to remember that it is just an idealistic conservative model. When taking into account energy losses due to air resistance, friction, damping more complicated behaviour is observed. This goes further when a second pendulum is attached creating double pendulum and the system is subjected to periodic excitation. Here a chaotic motion could be observed requiring more sophisticated mathematical tools for the analysis. In order to solve such models numerical methods are applied. [8] Numerical methods are time consuming and require considerably large computation power. However, the recent development of electronics increases the speed of the numerical operations and makes it possible to

perform calculations on computers available widely on the market.

This paper investigates the dynamics of double pendulum subjected to parametric horizontal periodic excitation. In following chapters theoretical background, mathematical model and results of the research are presented. The thesis is realised within the TEAM programme of Foundation for Polish Science, co-financed from European Union, Regional Development Fund.

1.1 A brief description of the investigated system

The investigated system is a double pendulum with horizontal parametric excitation. It consists of two limbs, where the first one is inelastic and the second elastic. The pendulum is subjected to horizontal excitation which means that the point of pendulum's suspension moves horizontally. More details about the system are presented in chapter 3.

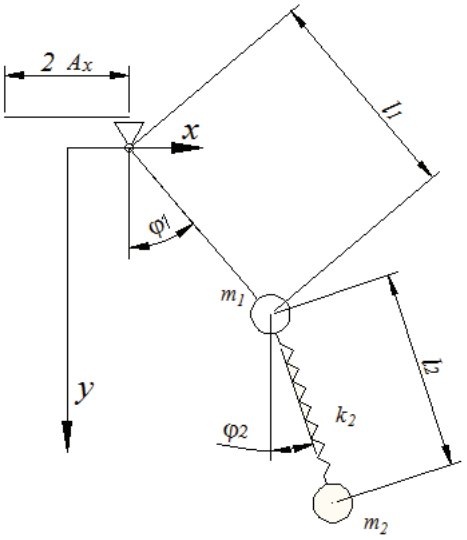

Figure 1.1: The scheme of the investigated system

1.2 The aim of the thesis

The aim of this thesis is to examine the dynamics of double pendulum subjected to horizontal excitation, which includes:

- creation of mathematical model
- writing own programs for solving and analysing ordinary differential equations
- analysing behaviour of the system basing on bifurcation diagrams for different control parameters
- analysing of the system basing on Poincaré maps and phase diagrams

Chapter 2

Theoretical background

In order to investigate dynamics of a nonlinear system such as double pendulum it is essential to get acquainted with the basic theory and tools concerning dynamics and analysis of the differential equations.

2.1 Lagrangian mechanics

Lagrangian mechanics describes motion in a mechanical system by means of the configuration space. The Lagrangian point of view allows to solve completely a series of important mechanical problems, including problems in the theory of small oscillations and in the dynamics of a rigid body. [2]

Definition 1. *(Constrain [9])*
Reasons for limitation of mass points system are called constrains.

Definition 2. *(Constrain equations [9])*
The limitation of movement of mass points can be presented analytically using formula having general form:

$$f_k(\vec{r_1}, \vec{r_2}, ..., \vec{r_n}) = 0 \quad (k = 1, 2, ..., p). \tag{2.1}$$

Definition 3. *(Degrees of freedom [9])*
Number f given by formula:

$$f = 3n - p \tag{2.2}$$

represents the number of degrees of freedom of the system of n mass points. It shows the number or independent variables from 3n coordinates x_1, y_1, z_1, ..., x_n, x_n, x_n bounded by p equations.

Definition 4. *(Generalised coordinates([1])*
Generalised coordinates are a set of convenient coordinates, usually independent of one another, used to describe the configuration of a particular system. If the system is subjected to some additional constraints that will result in some dependency between the generalised coordinates, the number of independent generalised coordinates defines the number of degrees of freedom.

After choosing proper generalised coordinates, it is possible to model the system equation defined below:

Definition 5. *(Second order Lagrange equations [5])*
For n degrees of freedom system, described by n generalised coordinates q_i, i = 1,2,...,n, second order Lagrange equations have the following form:

$$\frac{d}{dt}(\frac{\partial T}{\partial \dot{q}_i}) - \frac{\partial T}{\partial q_i} + \frac{\partial D}{\partial \dot{q}_i} + \frac{\partial V}{\partial q_i} = Q_i \tag{2.3}$$

where T is kinetic energy, V potential energy, D Rayleigh's dissipation function and Q_i is generalised external force acting on system. Q_i is given by formula:

$$Q_i = \sum_l F_l \frac{\partial r_l}{\partial q_i} + \sum_l M_l \frac{\partial \omega_l}{\partial \dot{q}_i} \tag{2.4}$$

where F_l and M_l are vectors of external forces and moments respectively, r_l is position vector in relation to point of force F_l application and ω_l is angular velocity of the system in relation to point of moment M_l application. The products in the above formula are scalar products.

2.2 Dynamical systems

Definition 6. *(Autonomous system [4])*
Consider the following system of differential equations:

$$\frac{dx}{dt} = f(x), \quad x(t_0) = x_0 \tag{2.5}$$

where $x \in D \subset \mathbb{R}^n, t \in \mathbb{R}^+$ and D is an open subset of $\mathbb{R}^n$. If the right hand side does not depend explicitly on time the system is called autonomous.

Definition 7. *(Non-autonomous system [4])*
Consider the following system of differential equations:

$$\frac{dx}{dt} = f(x,t), x(t_0) = x_0 \tag{2.6}$$

where $x \in D \subset \mathbb{R}^n, t \in \mathbb{R}^+$ and D is an open subset of $\mathbb{R}^n$. If the right hand side depends explicitly on time the system is called non-autonomous.

The example of non-autonomous system is a system oscillating with external excitation, where energy is delivered to the system.

The set D is called a phase space. [7]

Definition 8. *(Dynamical system [7])*
As a dynamical system, described by the system of equations (2.5)*, we call a mapping*

$$\phi : \mathbb{R} \times D \to \mathbb{R}^n \tag{2.7}$$

described by the solution $x(t)$ of the system of equations (2.5)*.*

Definition 9. *(Vector field [7])*
Function f, which is the right hand side of the (2.5) describes mapping f

$$f : D \to \mathbb{R}^n \tag{2.8}$$

defining vector field in $\mathbb{R}^n$.

Definition 10. *(Phase flow [7])*
Mapping

$$\phi_t : D \to \mathbb{R}^n \tag{2.9}$$

is called phase flow.

In [7] Kapitaniak defines phase space of a dynamic system as abstract space with orthogonal coordinates. Each coordinate describes variable needed to describe state of the system, (e.g. to describe the state of mass moving along a line, displacement x and velocity dx/dt are necessary). In general, phase space of the dynamic system described by the equation (2.5) is n-dimensional (equal to the dimension of the system).

For the system of equation given by general form

$$\frac{dx_i}{dt} = f_i(x), \quad i = 1, 2, ..., n \tag{2.10}$$

if $f_1(x) \neq 0$ then it is possible to take x_1 component of vector x as new independent variable. Then it yields to:

$$\frac{dx_2}{d_x 1} = \frac{f_2(x)}{f_1 x} ... \frac{dx_n}{d_x 1} = \frac{f_n(x)}{f_1 x}. \tag{2.11}$$

Definition 11. *(Trajectory [7])*
Solutions of the (2.11) *in phase space are called trajectory (orbit) of the system.*

Definition 12. *If there exists* $T > 0$ *such that*

$$f(x, t) = f(x, t + T) \tag{2.12}$$

for every x *and* t*, the system of equations* (2.6) *is called periodic with period* T*.*

Definition 13. *(Attractor [4])*
A specific subset A *in a phase space of equation* $f : \mathbb{R}^n \times \mathbb{R} \to \mathbb{R}^n, t \in \mathbb{R}$*, which is reached asymptotically by trajectory* $x(t)$*, when* $t \to \infty (t \to -\infty)$ *is called an attractor (repeller).*

2.3 Bifurcations

In English the verb 'bifurcate' is a formal word to express that something divides into two separate parts (e.g. river, road). This trivial example is somehow related to bifurcation in mathematical sense.

Definition 14. *(Bifurcation [7])*
Bifurcation occurs when the solution of nonlinear differential equation

$$\frac{dx}{dt} = f(x, \mu), \tag{2.13}$$

where

$$f : \mathbb{R}^n \times \mathbb{R} \to \mathbb{R}^n, \quad t, \mu \in \mathbb{R}, x \in \mathbb{R}^n$$

changes qualitatively its character along the change of parameter μ. The value of the parameter $\mu = \mu_c$, for which this change occurs is called a point of bifurcation.

The theory of bifurcation investigates the influence of parameter μ on the number or character of attractors. Bifurcations are divided into local and global. Local bifurcations occur in the neighbourhood of fixed points or periodic solution of the system. The bifurcation which requires global view on the phase space of the system and cannot be observed in the same neighbourhood as local is called global bifurcation. Below basic types of local bifurcations are considered.

2.3.1 Pitchfork bifurcation [7]

Consider a dynamical system described by equation:

$$\frac{dx}{dt} = ax - bx^3 \tag{2.14}$$

where $x \in \mathbb{R}$, a and b are real constants. The fixed points of (2.14) are

$$x = 0 \text{ for } x \in \mathbb{R}$$

and

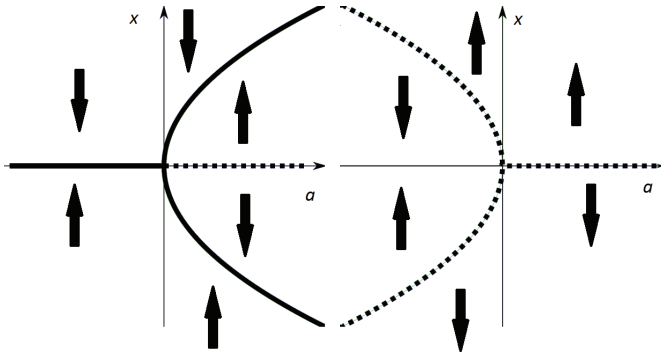

(a) Supercritical case (b) Subcritical case

Figure 2.1: Pitchfork bifurcations

$$x = \pm\sqrt{\tfrac{a}{b}} \text{ for } a, b \in \mathbb{R} \text{ and } \tfrac{a}{b} > 0$$

The fixed point $x = 0$ is stable when $b > 0$ and $a \leq 0$ or when $b < 0$ and $a < 0$. The fixed point x = 0 is unstable when $b > 0$ and $a > 0$. The fixed points $x = \pm\sqrt{\frac{a}{b}}$ are stable when $b > 0$ and $a > 0$. The fixed points $x = \pm\sqrt{\frac{a}{b}}$ are unstable when $b < 0$ and $a < 0$.

The case where $b > 0$ is called supercritical bifurcation as the qualitatively new solution occurs for $a > a_c$. The case where $b < 0$ is called subcritical bifurcation. Because of the shape of the plots presented in Figures 2.1 this type of the bifurcations is called pitchfork bifurcation.

2.3.2 Saddle-node bifurcation

Consider system described by the equation :

$$\frac{dx}{dt} = a - x^2 \tag{2.15}$$

where $x \in \mathbb{C}$
The fixed points of (2.15) are

$$x_{1,2} = \pm\sqrt{a} \tag{2.16}$$

For $a > 0$ there are two fixed points, for $a = 0$ one and for $a < 0$ fixed points do not exists.

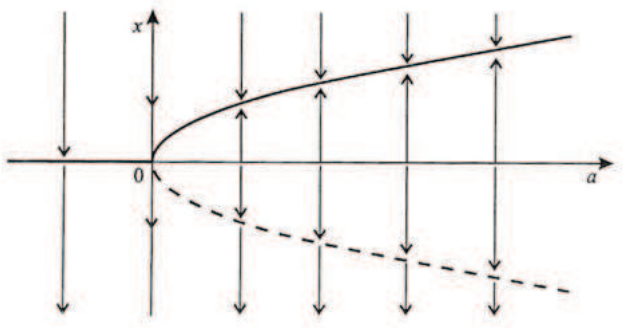

Figure 2.2: Saddle-node bifurcation [7]

The number of fixed points changes when parameter a goes through 0. So does the stability of the fixed points when parameter $x = \pm\sqrt{a}$ goes through 0. Such a bifurcation is called saddle-node bifurcation.

2.3.3 Hopf bifurcation [7]

Hopf bifurcation means loss of stability of fixed points resulting in emerging of the periodic solution.

Consider a system of differential equations

$$\begin{aligned} \frac{dx}{dt} &= -y + (a - x^2 - y^2)x \\ \frac{dy}{dt} &= x + (a - x^2 - y^2)y \end{aligned} \tag{2.17}$$

where $a \in \mathbb{R}$. Assuming

$$\frac{dx}{dt} = \frac{dy}{dt} = 0 \tag{2.18}$$

it is possible to show that $(x, y) = (0, 0)$ is a fixed point. Linearising equation (2.17) in the neighbourhood of fixed point

$$\begin{aligned} \frac{dx}{dt} &= -y + ax \\ \frac{dy}{dt} &= x + ay \end{aligned} \tag{2.19}$$

The solution of linearised system (2.19) is linear combination of functions

$$\begin{aligned} x(t) &= e^{\lambda t}u \\ y(t) &= e^{\lambda t}v \end{aligned} \tag{2.20}$$

fulfilling the equation

$$Au = su \tag{2.21}$$

where s is the eigenvalue, $u = [u, v]^T$ are eigen vectors and A is 2x2 matrix

$$\begin{bmatrix} a & -1 \\ 1 & a \end{bmatrix} \tag{2.22}$$

Then

$$0 = \det(A - sI) = \begin{vmatrix} a-s & -1 \\ 1 & a-s \end{vmatrix} = (a-s)^2 - 1 \tag{2.23}$$

$$s = a \pm i \tag{2.24}$$

The solution of linearised system is stable for $a < 0$ and unstable for $a > 0$. Transforming the system (2.17) into polar coordinates yields to:

$$(\frac{dr}{dt} + ir\frac{d\theta}{dt})e^{i\theta} \tag{2.25}$$

$$\frac{dr}{dt} = r(a-r)^2 \tag{2.26}$$
$$\frac{d\theta}{dt} = 1$$

$$r^2(t) = \begin{cases} \frac{ar_0^2}{r_0^2 + (a-r_0^2)e^{-2at}} & a \neq 0 \\ \frac{r_0^2}{1+2r_0^2 t} & a = 0 \end{cases} \tag{2.27}$$

For $a < 0$ all phase trajectories $x(t) \to 0$ when $t \to \infty$ and point $x(0,0)$ is attractor (see Figure 2.3a). For $a > 0$ point $x(0,0)$ becomes a repeller and new static solution appears, which is a limit-cycle (see fig. 2.3b).

$$x = \sqrt{}cos(t + \theta_0) \tag{2.28}$$
$$y = \sqrt{}sin(t + \theta_0)$$

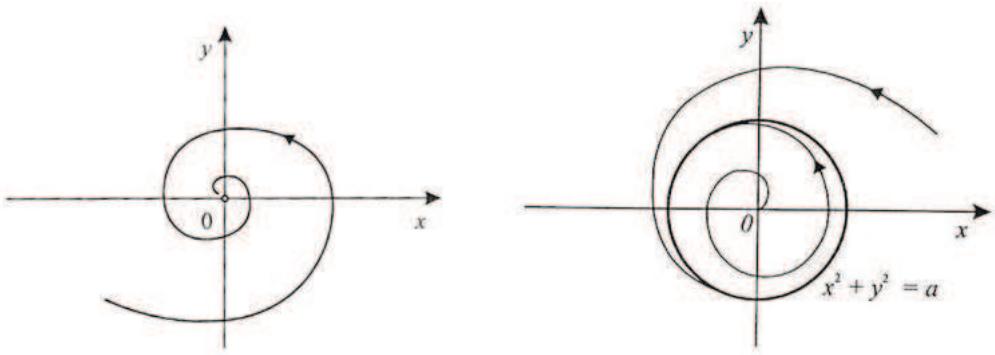

(a) Before Hopf bifurcation (b) After Hopf bifurcation

Figure 2.3: Behaviour of phase trajectories before and after the Hopf bifurcation [7]

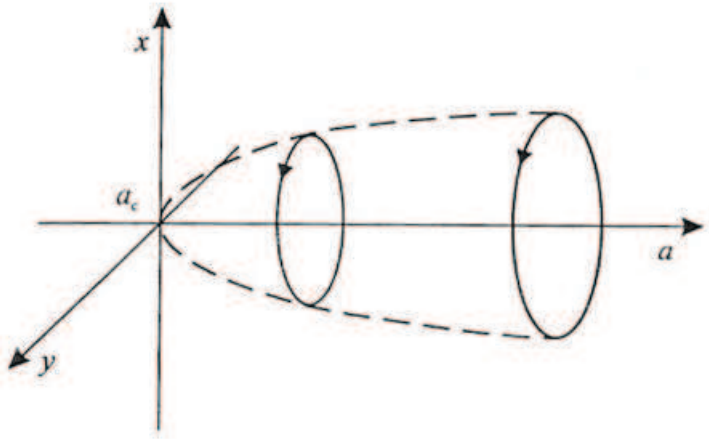

Figure 2.4: Limit-cycle as a result of Hopf bifurcation [7]

2.4 Route to chaos

There are 3 basic routes to chaos:

- Hopf bifurcation
- period doubling
- saddle-node bifurcation

2.4.1 Hopf bifurcation

In previous section 2.3, where Hopf bifurcation was described, it was mentioned that Hopf bifurcation causes limit cycle starting from a fixed point.After the first Hopf bifurcation system may undergo further Hopf bifurcations yielding to quasi-periodicity of the system and eventually a strange attractor can be created.

2.4.2 Period doubling

Consider dynamical system called logistic map

$$x_{n+1} = \mu x_n(1 - x_n) \tag{2.29}$$

that maps itself in range [0,1].
Bellow, a bifurcation diagram for logistic map is presented (see Figure 2.5), giving the information about the character of the system's behaviour The first period doubling occurs about $\mu = 3.0$,with period 2-atractor. Then for bigger values of μ , the period doubling occurs again and again , leading eventually to chaotic behaviour of the system.

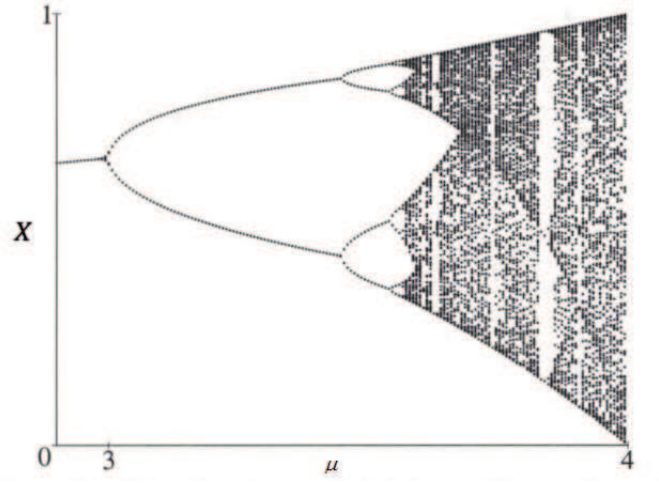

Figure 2.5: Bifurcation diagram for logistic map [3]

2.5 Visual representation of the system

The analysis of the dynamical system is performed using special graphs helping to interpret the character of system's behaviour. The pallet of tools includes time diagram, phase portrait, Poincaré map and bifurcation diagram.

2.5.1 Time diagram

The time diagram provides the information about the solution of the differential equation at the specific moment of time for respective variable describing the investigated system. It gives a brief view of the system properties. Should the plotted time range be long enough, it is possible to observe periodicity or irregular curves giving suspicion of quasi-periodicity or chaos. Further analysis requires more advanced tools.

2.5.2 Phase portrait

The solution of the system of differential equations evolves in time. In phase portrait the coordinates in phase space of point representing the solution of the system in given time instance are collected and projected on respective phase plains yielding to 2D plot. The shape of the phase portrait provides

information about the system behaviour. A close-loop shape indicates that the system is periodic. An irregular open shape may suggest chaos.

2.5.3 Poincaré map

Poincaré map is a powerful tool for describing the character of system behaviour. It was suggested by the French scientist, who contributed significantly to the analysis of the differential equations. Using Poincaré map, it is possible to recognise whether the system is periodic, quasi periodic or chaotic. The definition of Poincaré map depends on whether the system is autonomous or non-autonomous. As the system investigated in this thesis is non-autonomous, only the definition of Poincaré map for non-autonomous system is presented. For a time periodic n dimensional non-autonomous system with period T which can be transformed into an (n+1) dimensional order autonomous system in the cylindrical phase space $\mathbb{R}^n \times S^1$ the Poincaré map can be defined in the following way.

Definition 15. *(Poincaré map [6])*
Let one consider the n-dimensional surface $S \subset \mathbb{R}^n \times S^1$

$$S = (x, \theta) \subset \mathbb{R} \times S^n : \theta = \theta_0 \tag{2.30}$$

when after every period T*, the orbit* $x(t)$ *intersects* S *(see Figure 2.6). The resulting map* $P : S \to S(\mathbb{R}^n \to \mathbb{R}^n)$ *which maps* $x(t) \to x(t+T)$ *is a Poincaré map*

The analysis of Poincaré maps helps to determine the character of the system behaviour. If the system has periodic behaviour, then on the Poincaré map single point is plotted. Should the system be quasi-periodic, the obtained map presents the closed loop. Finally, if on the Poincaré map irregular points are plotted, it suggests chaotic behaviour.

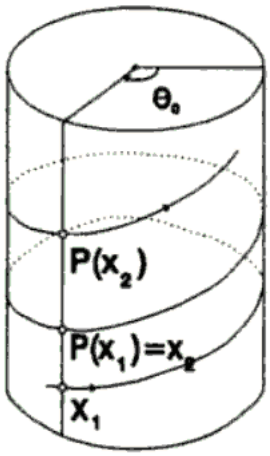

Figure 2.6: Surface S [7]

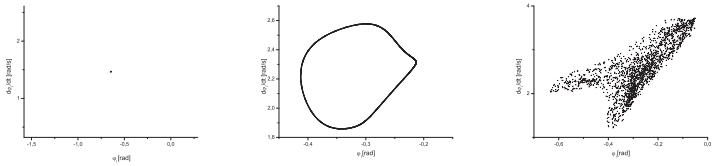

(a) periodic (b) quasi-periodic (c) chaotic

Figure 2.7: Poincaré maps for different behaviours of the system

2.5.4 Bifurcation diagrams

Bifurcations were discussed in section 2.3. In fact, bifurcation diagram presents multiply Poincaré maps for different value of bifurcation parameter. The bifurcation parameter is on the x-axis, while on the y-axis the selected variable describing the ODE system. The points on the bifurcation diagram are projection of Poincaré map of the respective variable for specific value of bifurcation parameter. Therefore the pattern for determining the character of the system behaviour is the same. When for specific value of bifurcation parameter there is only one point on the diagram, the system is periodic. Multiply points for specific value of bifurcation parameter distributed irregular (regular) indicates chaos (quasi-periodicity). The bifurcation diagram shows the behaviour of the system in the wide range of

bifurcation parameter. When the bifurcation parameter is increased in each successive iteration the bifurcation is called forward. Reaching the end of the interval of the bifurcation parameter the last saved results are used as initial parameters for backward bifurcation (i.e. the bifurcation parameter is decreased until it reaches the beginning of the interval). Using forward and backward bifurcation diagrams, it is possible to check if the solution follows the same attractor or there exist another solution of the system.

Chapter 3

Mathematical model

Before investigating any dynamics system, it is essential to provide a model, which describes all relevant physical properties in language of mathematics. With the application of Lagrangian mechanics, a general model for double elastic pendulum with elliptical excitation is derived, followed by special case for double pendulum excited horizontally, with only one elastic limb. As a result, a set of ordinary differentials equations is obtained, which are later used in computer program.

3.1 General model

Consider a 2D double pendulum with elastic limbs. The limbs of the pendulum are: assumed to be mass-less with point masses m_1 and m_2 attached to end of each limb respectively, elastic (i.e. treated as swinging springs with spring constants k_1 and k_2). Additional parameters are : the rest lengths of limbs l_{r1} , l_{r2}, damping coefficients on connecting nodes c_1 , c_2 and on springs c_3, c_4. The system has 4 degrees of freedom.

The elliptical movement of the pendulum's suspension can be resolve into horizontal W_x and vertical W_y displacements, where amplitudes A_x, A_y are respective radiuses of the ellipse, ω_x, ω_y are frequencies of excitations and t is time :

$$W_x = A_x \cos \omega_x t \tag{3.1}$$

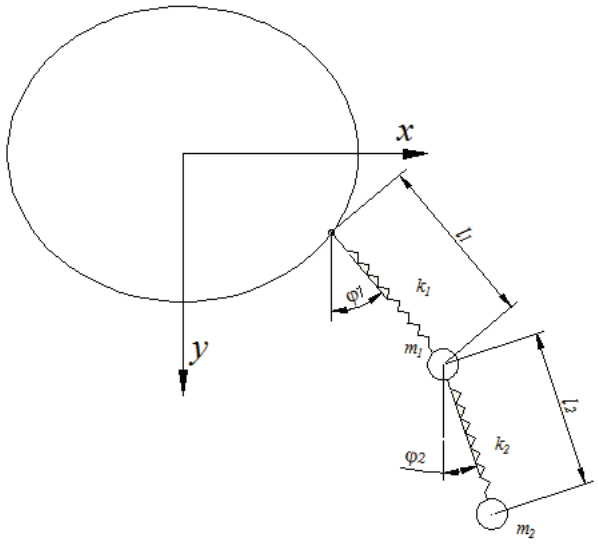

Figure 3.1: Scheme of double elastic pendulum with elliptical excitation

$$W_y = A_y \sin \omega_y t \tag{3.2}$$

The successive derivatives of W_x used in later calculations are :

$$\dot{W}_x = -A_x \omega_x \sin \omega_x t \tag{3.3}$$

$$\dot{W}_y = A_y \omega_y \cos \omega_y t \tag{3.4}$$

$$\ddot{W}_x = -A_x {\omega_x}^2 \cos \omega_x t \tag{3.5}$$

$$\ddot{W}_y = -A_y {\omega_y}^2 \sin \omega_y t \tag{3.6}$$

The origin of the Cartesian coordinate system is placed on the node connecting pendulum with suspension, for the displacement $W_x = 0$ and $W_y = 0$. The x-axis is oriented rightwards and y-axis downwards.

In the state of rest both springs are extended by the loads (see Figure 3.2b) . Therefore their initial lengths l_{01} and l_{02} are:

$$l_{01} = l_{r1} + (m_1 + m_2)\frac{g}{k_1} \tag{3.7}$$

$$l_{02} = l_{r2} + m_2 \frac{g}{k_2} \tag{3.8}$$

While swinging, springs elongate further and their lengths are l_1 and l_2. The motion of the pendulum is modelled with Lagrangian approach using

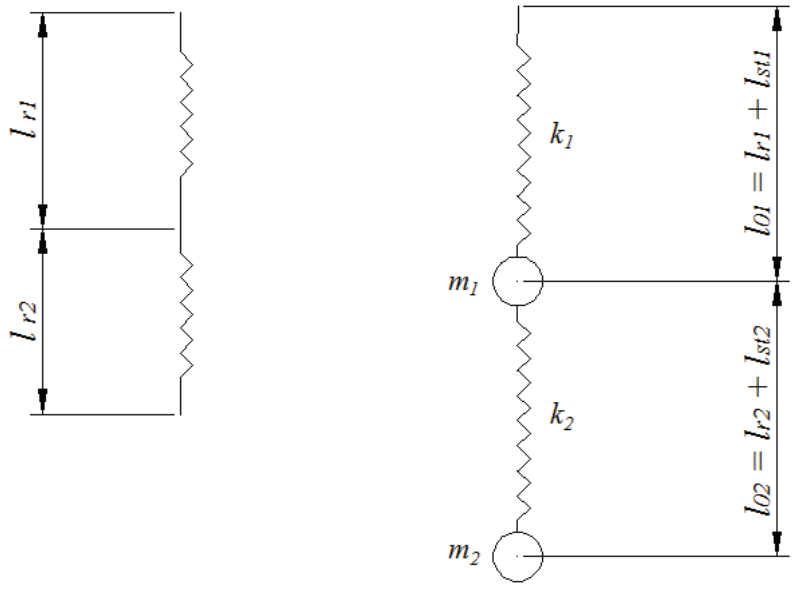

(a) Unloaded pendulum (b) Loaded pendulum

Figure 3.2: Initial states of pendulum

φ_1, φ_2, l_1 and l_2 (see Figure **??**) as generalised coordinates. The derivation of terms in (2.3) is as follows:

$$\vec{r_1} = (l_1 \sin\varphi_1 + W_x)\hat{i} + (l_1 \cos\varphi_1 + W_y)\hat{j} \tag{3.9}$$

$$\vec{r_2} = (l_1 \sin\varphi_1 + W_x + l_2 \sin\varphi_2)\hat{i} + (l_1 \cos\varphi_1 + W_y + l_2 \cos\varphi_2)\hat{j} \tag{3.10}$$

where $\vec{r_1}$ and $\vec{r_2}$ are position vectors of each respective mass. Derivation of (3.9) and (3.10) yields to:

$$\dot{\vec{r_1}} = (\dot{l_1} \sin\varphi_1 + l_1\dot{\varphi_1} \cos\varphi_1 + \dot{W_x})\hat{i} + (\dot{l_1} \cos\varphi_1 - l_1\dot{\varphi_1} \sin\varphi_1 + \dot{W_y})\hat{j} \tag{3.11}$$

$$\begin{aligned}\dot{\vec{r_2}} = (&\dot{l_1} \sin\varphi_1 + l_1\dot{\varphi_1} \cos\varphi_1 + \dot{W_x} + \dot{l_2} \sin\varphi_2 + l_2\dot{\varphi_2} \cos\varphi_2)\hat{i} \\ &+(\dot{l_1} \cos\varphi_1 - l_1\dot{\varphi_1} \sin\varphi_1 + \dot{W_y} + \dot{l_2} \cos\varphi_2 - l_2\dot{\varphi_2} \sin\varphi_2)\hat{j}\end{aligned} \tag{3.12}$$

Eventually squares of velocities (3.11) (3.12) are obtained :

$$\begin{aligned}{v_1}^2 = &\dot{l_1}^2 + \dot{W_x}^2 + \dot{W_y}^2 + {l_1}^2\dot{\varphi_1}^2 + 2\dot{l_1}\dot{W_x} \sin\varphi_1 \\ &+2l_1\dot{\varphi_1}\dot{W_x} \cos\varphi_1 + 2\dot{l_1}\dot{W_y} \cos\varphi_1 - 2l_1\dot{\varphi_1}\dot{W_y} \sin\varphi_1\end{aligned} \tag{3.13}$$

$$
\begin{aligned}
{v_2}^2 = 2l_1\dot{\varphi_1}\dot{W_x}\cos\varphi_1 - 2l_1\dot{\varphi_1}\dot{W_y}\sin\varphi_1 + 2\dot{l_1}\dot{W_x}\sin\varphi_1 + 2\dot{l_1}\dot{W_y}\cos\varphi_1 \\
+\dot{l_1}^2 + \dot{W_x}^2 + \dot{W_y}^2 + {l_1}^2{\dot{\varphi_1}}^2 + 2l_2\dot{W_x}\dot{\varphi_2}\cos\varphi_2 - 2l_2\dot{W_y}\dot{\varphi_2}\sin\varphi_2 + \\
+2\dot{l_1}\dot{l_2}\cos(\varphi_1-\varphi_2) + 2l_1l_2\dot{\varphi_1}\dot{\varphi_2}\cos(\varphi_1-\varphi_2) + \dot{l_2}^2 + 2\dot{l_1}l_2\dot{\varphi_2}\sin(\varphi_1-\varphi_2) \\
+{l_2}^2{\dot{\varphi_2}}^2 - 2l_1\dot{l_2}\dot{\varphi_1}\sin(\varphi_1-\varphi_2) + 2\dot{l_2}\dot{W_x}\sin\varphi_2 + 2\dot{l_2}\dot{W_y}\cos\varphi_2
\end{aligned}
\tag{3.14}
$$

Having (3.13) and (3.14), it is possible to calculate kinetic energy T of the system.

$$T = \frac{1}{2}m_1{v_1}^2 + \frac{1}{2}m_2{v_2}^2 \tag{3.15}$$

The potential energy V of the system is given by the following formula :

$$
\begin{aligned}
V = m_1gl_1(1-\cos\varphi_1) + m_2g(l_1(1-\cos\varphi_1) + l_2(1-\cos\varphi_2)) + \\
+\frac{k_1}{2}(l_1-l_{01})^2 + \frac{k_2}{2}(l_2-l_{02})^2
\end{aligned}
\tag{3.16}
$$

The last element to calculate is the Rayleigh's dissipation function D.

$$D = \frac{1}{2}(c_1{\dot{\varphi_1}}^2 + c_2(\dot{\varphi_2}-\dot{\varphi_1})^2 + c_3\dot{l_1}^2 + c_4\dot{l_2}^2) \tag{3.17}$$

Applying (3.15) (3.16) and (3.17) in (2.3) and using q as generalised coordinate

$$q = \begin{pmatrix} \varphi_1 \\ \varphi_2 \\ l_1 \\ l_2 \end{pmatrix} \tag{3.18}$$

one obtains a four-dimensional system of second order Lagrange's equations. The system of equations is transformed, so that every product without acceleration of generalised coordinate is on the right-hand side. It yields to matrix form :

$$M\ddot{q} = R \tag{3.19}$$

where M is mass matrix and R right-hand side matrix

$$M = \begin{bmatrix} (m_1+m_2)l_1^2 & m_2 l_1 l_2 \cos(\varphi_1-\varphi_2) & 0 & -m_2 l_1 \sin(\varphi_1-\varphi_2) \\ m_2 l_1 l_2 \cos(\varphi_1-\varphi_2) & m_2 l_2^2 & m_2 l_2 \sin(\varphi_1-\varphi_2) & 0 \\ 0 & m_2 l_2 \sin(\varphi_1-\varphi_2) & m_1+m_2 & m_2 \cos(\varphi_1-\varphi_2) \\ -m_2 l_1 \sin(\varphi_1-\varphi_2) & 0 & m_2 \cos(\varphi_1-\varphi_2) & m_2 \end{bmatrix} \tag{3.20}$$

$$\ddot{q} = \begin{pmatrix} \ddot{\varphi}_1 \\ \ddot{\varphi}_2 \\ \ddot{l}_1 \\ \ddot{l}_2 \end{pmatrix} \tag{3.21}$$

$$R = \begin{bmatrix} (m_1+m_2)l_1(\ddot{W}_y \sin\varphi_1 - \ddot{W}_x \cos\varphi_1 - 2\dot{l}_1\dot{\varphi}_1 - g\sin\varphi_1) - m_2 l_1 l_2 \dot{\varphi}_2^2 \sin(\varphi_1-\varphi_2) - 2m_2 l_1 \dot{l}_2 \dot{\varphi}_2 \cos(\varphi_1-\varphi_2) - c_1\dot{\varphi}_1 + c_2(\dot{\varphi}_2-\dot{\varphi}_1) \\ -m_2 l_2(2\dot{\varphi}_2\dot{l}_2 + \ddot{W}_x\cos\varphi_2 - \ddot{W}_y\sin\varphi_2 + g\sin\varphi_2 + 2\dot{l}_1\dot{\varphi}_1\cos(\varphi_1-\varphi_2) - l_1\ddot{\varphi}_1^2\sin(\varphi_1-\varphi_2)) + c_2(\dot{\varphi}_1-\dot{\varphi}_2) \\ -(m_1+m_2)(\ddot{W}_x\sin\varphi_1 + \ddot{W}_y\cos\varphi_1 - l_1\dot{\varphi}_1^2 + g(1-\cos\varphi_1)) + m_2(l_2\dot{\varphi}_2^2\cos(\varphi_1-\varphi_2) - 2\dot{l}_2\dot{\varphi}_2\sin(\varphi_1-\varphi_2)) + k_1(l_{01}-l_1) - c_3\dot{l}_1 \\ m_2(2\dot{l}_1\dot{\varphi}_1\sin(\varphi_1-\varphi_2) - \ddot{W}_x\sin\varphi_2 - \ddot{W}_y\cos\varphi_2 + l_1\dot{\varphi}_1^2\cos(\varphi_1-\varphi_2) + l_2\ddot{\varphi}_2^2 - g(1-\cos\varphi_2)) + k_2(l_{02}-l_2) - c_4\dot{l}_2 \end{bmatrix} \tag{3.22}$$

3.2 Investigated case

In section 3.1 a general model for the system of double spring pendulum with elliptical excitation was proposed. Here a special case is investigated with only horizontal excitation and inelastic first limb of pendulum. The derivation of equations is done using the same approach as in section 3.1. The aim is to check whether this case satisfies relations for the general model.

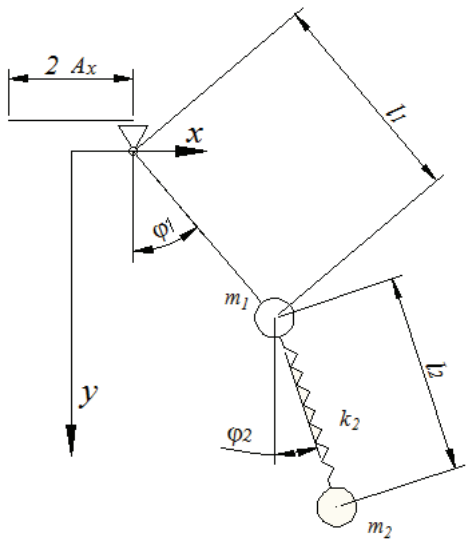

Figure 3.3: Scheme of the investigated system

The investigated model consists of 2D double pendulum with horizontal periodic excitation. The system has 3 degrees of freedom. The limbs of the pendulum are assumed to be mass-less with point masses m_1 and m_2 attached to the end of each limb respectively. The first rod is inextensible and taut with constant length l_1, while the second is treated as elastic pendulum with rest length l_{r2} and spring constant k_2. Additionally, due to friction on connecting nodes damping is included to the model by respective viscous damping coefficients c_1, c_2 and c_4 as damping coefficient of the spring. The suspension of the pendulum is moving horizontally with periodic displacement $W_x(t)$.

$$W_x = A_x \cos \omega_x t \tag{3.23}$$

where t is time, A_x is the amplitude and ω_x frequency of excitation. The successive derivatives of W_x used in later calculations are :

$$\dot{W}_x = -A_x \omega_x \sin \omega_x t \tag{3.24}$$

$$\ddot{W}_x = -A_x {\omega_x}^2 \cos \omega_x t \tag{3.25}$$

In the state of rest spring is extended by the load (see Figure 3.4). Therefore, its initial length l_{02}:

$$l_{02} = l_{r2} + m_2 \frac{g}{k_2} \tag{3.26}$$

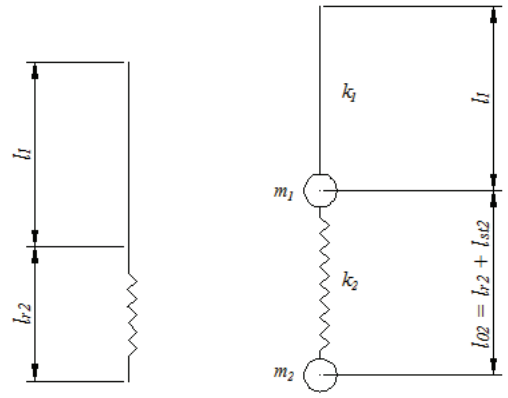

(a) Unloaded pendulum (b) Loaded pendulum

Figure 3.4: Initial states of pendulum

Following steps in section 3.1 one obtains:

$$\vec{r_1} = (l_1 \sin \varphi_1 + W_x)\hat{i} + (l_1 \cos \varphi_1)\hat{j} \tag{3.27}$$

$$\vec{r_2} = (l_1 \sin \varphi_1 + W_x + l_2 \sin \varphi_2)\hat{i} + (l_1 \cos \varphi_1 + l_2 \cos \varphi_2)\hat{j} \tag{3.28}$$

$$\dot{\vec{r_1}} = (l_1 \dot{\varphi_1} \cos \varphi_1 + \dot{W}_x)\hat{i} + (-l_1 \dot{\varphi_1} \sin \varphi_1)\hat{j} \tag{3.29}$$

$$\dot{\vec{r_2}} = (l_1 \dot{\varphi_1} \cos \varphi_1 + \dot{W}_x + \dot{l_2} \sin \varphi_2 + l_2 \dot{\varphi_2} \cos \varphi_2)\hat{i} + (-l_1 \dot{\varphi_1} \sin \varphi_1 + \dot{l_2} \cos \varphi_2 - l_2 \dot{\varphi_2} \sin \varphi_2)\hat{j} \tag{3.30}$$

$$v_1^2 = l_1^2 \dot{\varphi_1}^2 + 2 l_1 \dot{W}_x \dot{\varphi}_1 \cos\varphi_1 + \dot{W}_x^2 \tag{3.31}$$

$$\begin{aligned} v_2^2 = \; & l_1^2 \dot{\varphi_1}^2 + 2 l_1 \dot{W}_x \dot{\varphi}_1 \cos\varphi_1 + \dot{W}_x^2 + \dot{l_2}^2 + l_2^2 \dot{\varphi_2}^2 + 2\dot{W}_x (l_2 \dot{\varphi}_2 \cos\varphi_2 + \dot{l}_2 \sin\varphi_2) \\ & + 2 l_1 (l \dot{\varphi}_1 \dot{\varphi}_2 \cos(\varphi_1 - \varphi_2) - \dot{l}_2 \dot{\varphi}_1 \sin(\varphi_1 - \varphi_2)) \end{aligned} \tag{3.32}$$

Knowing (3.31) and (3.32), it is possible to calculate kinetic energy T:

$$T = \frac{1}{2} m_1 v_1^2 + \frac{1}{2} m_2 v_2^2 \tag{3.33}$$

Potential energy V is defined as follows

$$V = m_1 g l_1 (1 - \cos\varphi_1) + m_2 g (l_1 (1 - \cos\varphi_1) + l_2 (1 - \cos\varphi_2)) + \frac{k_2}{2} (l_2 - l_{02})^2 \tag{3.34}$$

and the Rayleigh's dissipation function

$$D = \frac{1}{2} (c_1 \dot{\varphi_1}^2 + c_2 (\dot{\varphi}_2 - \dot{\varphi}_1)^2 + c_4 \dot{l_2}^2) \tag{3.35}$$

Solving (2.3) using(3.33) (3.34) and (3.35) and q as generalised coordinate

$$q = \begin{pmatrix} \varphi_1 \\ \varphi_2 \\ l_2 \end{pmatrix} \tag{3.36}$$

After transformations similar to that in section 3.1 three-dimensional system of equations is obtained presented below in matrix form

$$M \ddot{q} = R \tag{3.37}$$

Pre-multiplying both sides of the (3.37) one obtains

$$\ddot{q} = M^{-1} R \tag{3.38}$$

All operations on the right hand side of the (3.38) are performed by computer program.

$$M = \begin{bmatrix} (m_1+m_2)l_1^2 & m_2 l_1 l_2 \cos(\varphi_1-\varphi_2) & -m_2 l_1 \sin(\varphi_1-\varphi_2) \\ m_2 l_1 l_2 \cos(\varphi_1-\varphi_2) & m_2 l_2^2 & 0 \\ -m_2 l_1 \sin(\varphi_1-\varphi_2) & 0 & m_2 \end{bmatrix} \tag{3.39}$$

$$\ddot{q} = \begin{pmatrix} \ddot{\varphi}_1 \\ \ddot{\varphi}_2 \\ \ddot{l}_2 \end{pmatrix} \tag{3.40}$$

$$R = \begin{bmatrix} -(m_1+m_2)l_1(\ddot{W}_x \cos\varphi_1 + g\sin\varphi_1) - m_2 l_1 l_2 \dot{\varphi}_2^2 \sin(\varphi_1-\varphi_2) - 2m_2 l_1 \dot{l}_2 \dot{\varphi}_2 \cos(\varphi_1-\varphi_2) - c_1\dot{\varphi}_1 + c_2(\dot{\varphi}_2-\dot{\varphi}_1) \\ -m_2 l_2(2\dot{\varphi}_2\dot{l}_2 + \ddot{W}_x \cos\varphi_2 + g\sin\varphi_2 - l_1\dot{\varphi}_1^2 \sin(\varphi_1-\varphi_2)) + c_2(\dot{\varphi}_1-\dot{\varphi}_2) \\ m_2(-\ddot{W}_x \sin\varphi_2 + l_1\dot{\varphi}_1^2 \cos(\varphi_1-\varphi_2) + l_2\dot{\varphi}_2^2 - g(1-\cos\varphi_2)) + k_2(l_{02}-l_2) - c_4\dot{l}_2 \end{bmatrix} \tag{3.41}$$

Chapter 4

Numerical analysis

In this chapter results of the numerical analysis of the double pendulum with parametric horizontal excitation are presented. The mathematical model used in the analysis is described in 3.2. The analysis was performed by author's software written in C.

4.1 Program

For purpose of the thesis a special program was written in C language and compiled by GCC compiler. The program uses 1.15 version of GNU Scientific Library (GSL) and is designed to work with UNIX based operating systems. The system of second order differential equations presented in chapter 3.2 is reduced to ordinary different and solved using GSL built-in explicit 4th order Runge-Kutta method with fixed time step. The time step is $T/3600$ where T is the period of excitation. Variations of program using the same integrating core were written depending on the desired output (phase diagram, Poincaré map, bifurcation diagram). The reason why C programming language was chosen for that task was determined by the GSL library itself, as it is written in C. Although there exist wrapping classes for GSL in C++ or Java, it was better to stick to the original language of the library. One of the most important factors which was taken into con-

sideration while designing the program was the optimisation, so that the execution time is low. Therefore, software is executed from the command shell. The program is called along with the value of the initial conditions. Should multiple simulations be performed, it is possible to write bash script, enabling automatic launch of one simulation after another. For computers with multi-cores CPU it is advised to launch simulations parallel (one simulation per core), so that the available computation power is maximised. The execution time of single simulation remains the same, however the CPU load reaches it maximum and no other activity on the PC is advised.

4.2 Simulation

It was important to choose parameters of the investigated system in such a manner that they correspond to sensible values from engineering point of view . Therefore, the following parameter values were assumed:

$$m_1 = 2 \quad kg$$

$$m_2 = 4 \quad kg$$

$$l_1 = 0.75 \quad m$$

$$l_{r2} = 0.7 \quad m$$

$$A_x = 0.3 \quad m$$

The spring coefficient k_2 is analysed for 2 different values

$$k_2 = 500 \quad N/m$$

$$k_2 = 1000 \quad N/m$$

The damping coefficients c_1, c_2 and c_4 are set, so thatthe system is underdamped.

$$c_1 = 0.04 \cdot m_1 \sqrt{g{l_1}^3} \quad kgm^2/s \tag{4.1}$$

$$c_2 = 0.02 \cdot m_2 \sqrt{g{l_{02}}^3} \quad kgm^2/s \tag{4.2}$$

$$c_4 = 0.1 \cdot 2\sqrt{m_2 k_2} \quad kg/s \tag{4.3}$$

The simulation starts with following initial conditions:

$$\varphi_1 = \frac{\pi}{6} \quad rad$$

$$\dot{\varphi_1} = 0 \quad rad/s$$

$$\varphi_2 = \frac{\pi}{8} \quad rad$$

$$\dot{\varphi_2} = 0 \quad rad/s$$

$$l_2 = l_{02} + 0.01 \quad m$$

$$\dot{l_2} = 0 \quad m/s$$

The data are saved after 250 periods of excitation when the system stabilises. For the bifurcation diagram data from 100 periods of excitation is recorded.

4.3 Results

In order to find out the behaviour of the system depending on the angular frequency ω_x forward and backward bifurcation over interval [0.1, 10] Hz is performed. The bifurcation parameter ω_x is changed with step 0.05. At first the system is investigated for spring coefficient $k_2 = 500$ N/m and then $k_2 = 1000$ N/m. Since the behaviour on the bifurcation diagrams for each respective generalise coordinate is similar, only selected bifurcation diagrams are presented.

The analysis of Figures 4.1 and 4.2 reveals different kinds of oscillatory motion in terms of periodicity. From small value of ω_x a periodic motion is observed. At 4.7 Hz the period of oscillations doubles, while in 5.2 Hz solution hoops to another attractor with period-3, followed again by zone of singular period oscillations ($\omega_x > 6$ Hz). The change of attractor occurs also in 8 Hz. Eventually, the system reaches chaos for $\omega_x > 9.2$ Hz. From backward bifurcation diagram it can be observed that the system follows

slightly different attractor, which implies coexistence of attractors. Figure 4.3 presents the bifurcation in range [2.2, 3.0] Hz with bifurcation parameter step 0.005. In that range the system remains periodic. Figure 4.4 also presents detailed bifurcation on the interval [4.6, 6.0] Hz, where it is possible to observe several change of the attractor. The double period attractor is followed by singular period attractor and then it goes to period-3 attractor. Figure 4.5 shows detailed view on interval 7.9 Hz $< \omega_x <$ 8.1 Hz. The applied bifurcation parameter step was 0.001. Here hooping between attractors is observed, but in detailed calculations the solution goes to different attractor than on the general view (Figure 4.1).

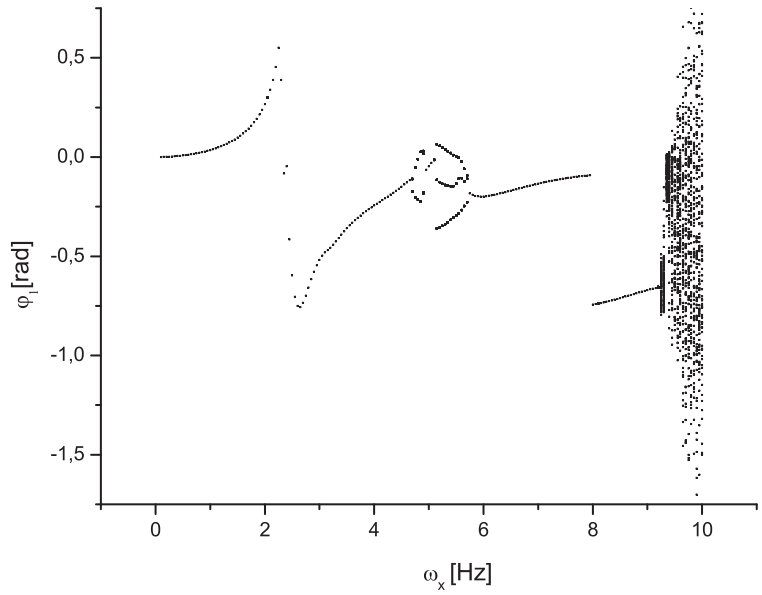

Figure 4.1: Forward bifurcation diagram for φ_1 with $k_2 = 500$ N/m

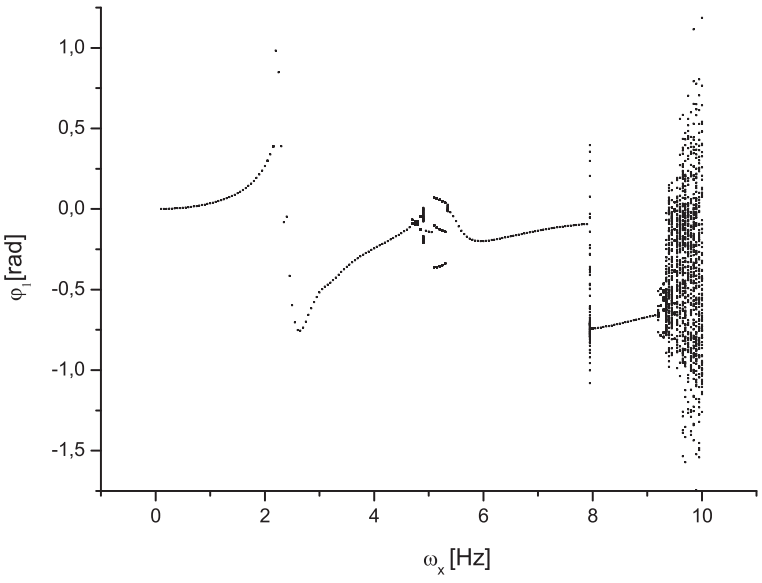

Figure 4.2: Backward bifurcation diagram for φ_1 with $k_2 = 500$ N/m

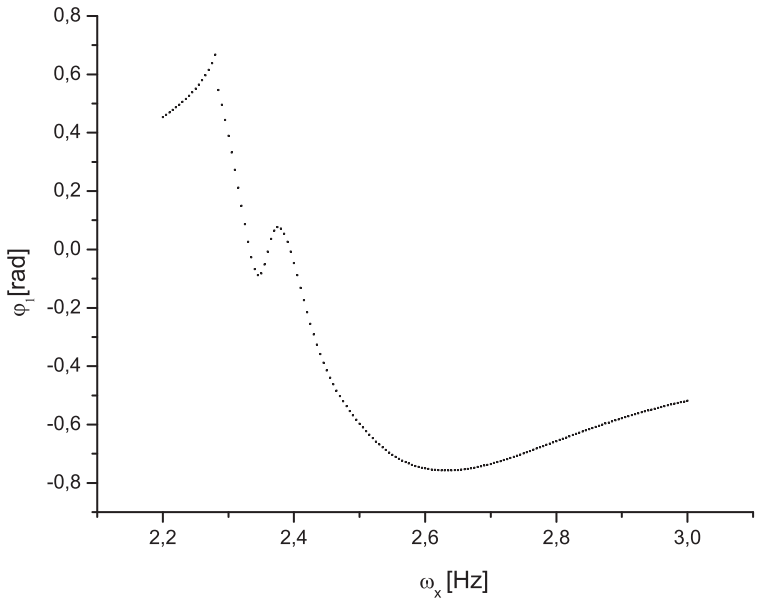

Figure 4.3: Forward bifurcations for $2.2Hz \leq \omega_x \leq 3Hz$ with 0.005 step

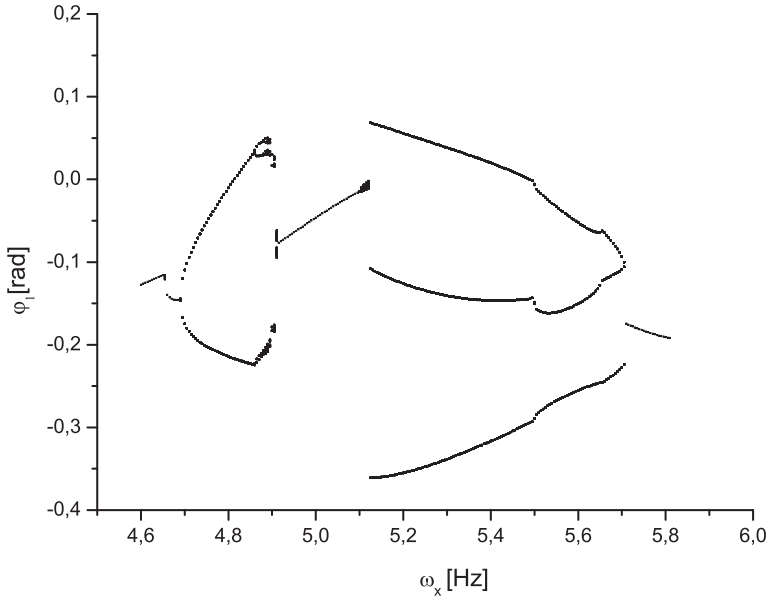

Figure 4.4: Backward bifurcations for $4.6Hz \leq \omega_x \leq 6.0Hz$ with 0.005 step

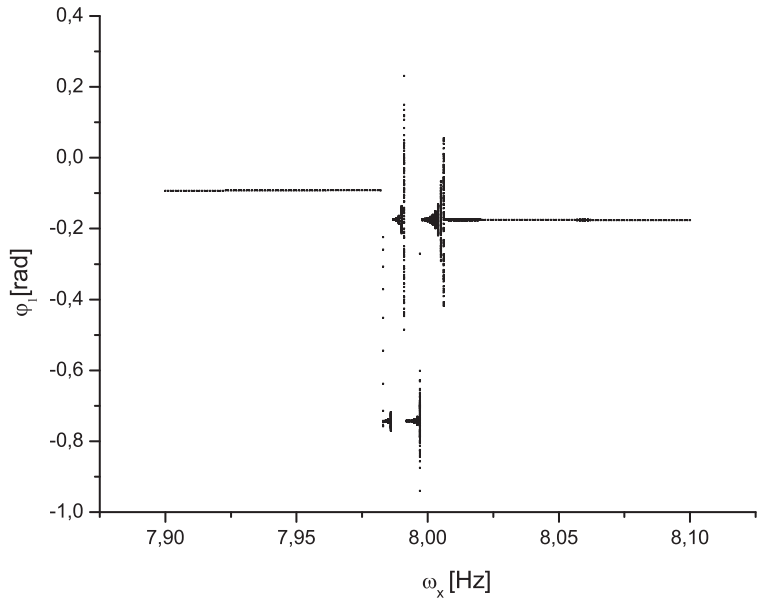

Figure 4.5: Forward bifurcations for $7.9Hz \leq \omega_x \leq 8.1Hz$ with 0.001 step

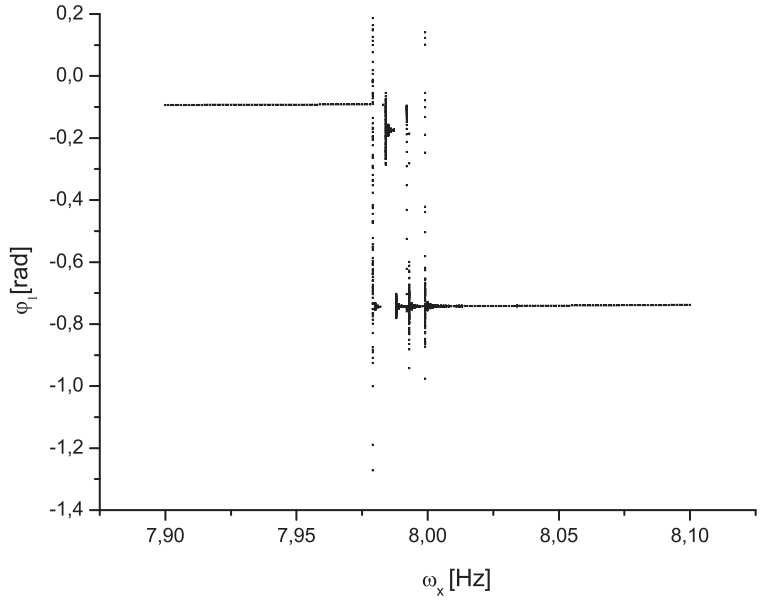

Figure 4.6: Backward bifurcations for $8.1Hz \geq \omega_x \geq 7.9Hz$ with 0.001 step

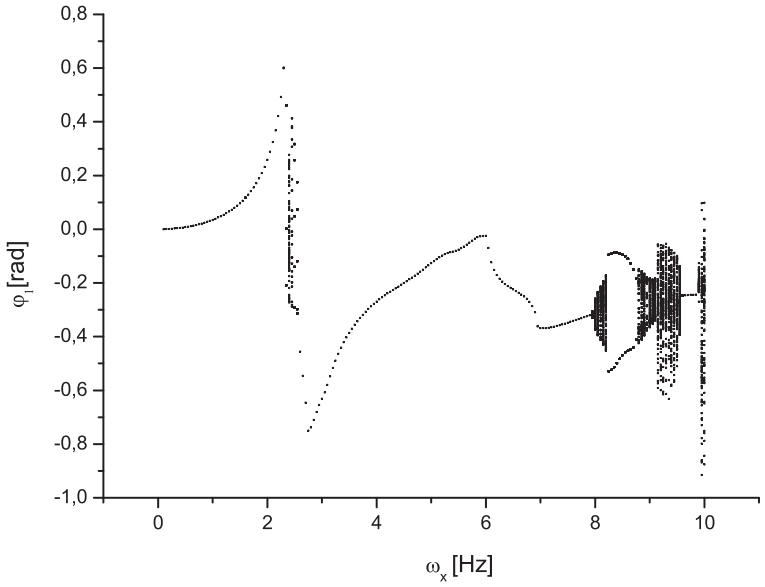

Figure 4.7: Forward bifurcation diagram for φ_1 with $k_2 = 1000$ N/m

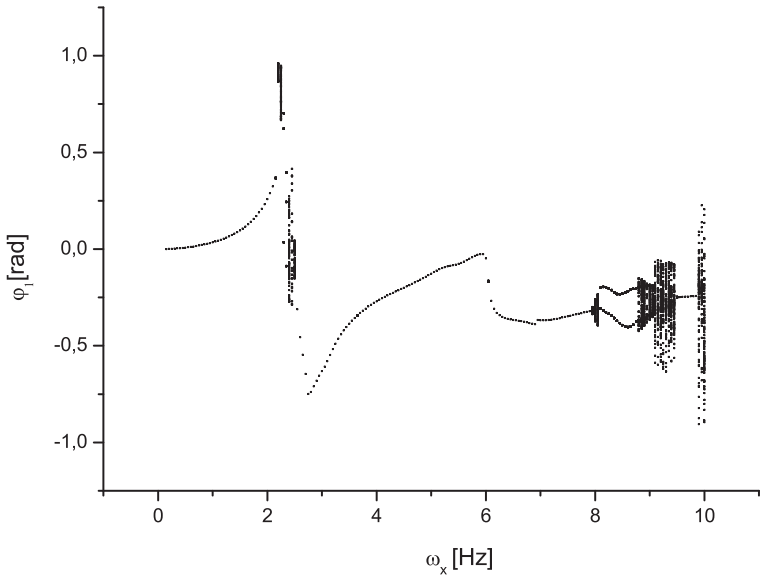

Figure 4.8: Backward bifurcation diagram for φ_1 with $k_2 = 1000$ N/m

From the bifurcation diagrams in Figures 4.7 and 4.8 it is possible to observe similar regions like for the system with $k_2 = 500$ N/m. However, there are some remarkable differences such as lack of period doubling or period-3 attractors about 5 Hz. What is more, the appearance of quasi-periodic zone about $\omega_x = 2.4$ Hz is observed. The quasi-periodicity occurs also about $\omega_x = 8$ Hz, but in 8.25 Hz it changes to double period. About $\omega_x = 8.7$ Hz the system is again quasi periodic only to become chaotic in $\omega_x = 9.15$ Hz. There exist singular period periodic windows. As in previous system the downward bifurcation follows slightly different attractor but behaviour of the system is similar.

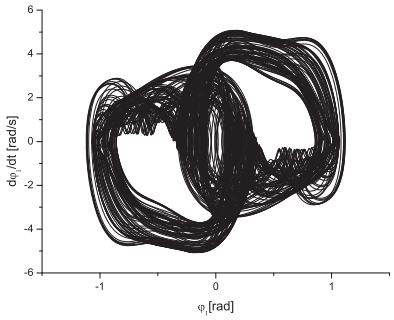

(a) Phase portrait $\omega_x = 2.4$ Hz

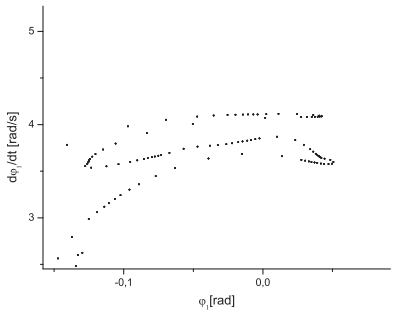

(b) Poincaré map $\omega_x = 2.4$ Hz

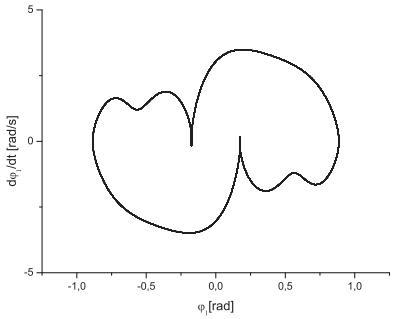

(c) Phase portrait $\omega_x = 2.7$ Hz

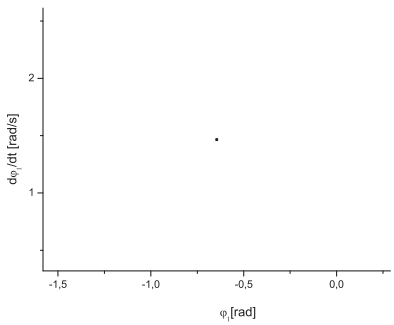

(d) Poincaré map $\omega_x = 2.7$ Hz

Figure 4.9: Phase portraits and Poincaré maps for different ω_x for $k_2 = 1000$ N/m

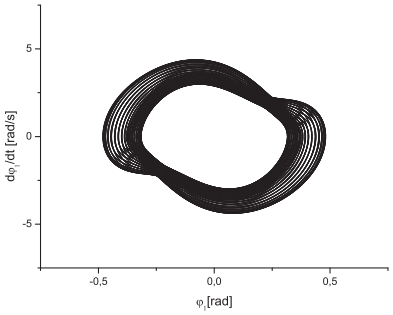

(a) Phase portrait $\omega_x = 8.1$ Hz

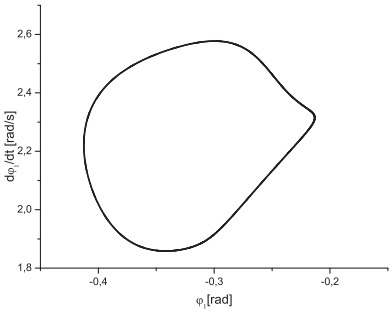

(b) Poincaré map $\omega_x = 8.1$ Hz

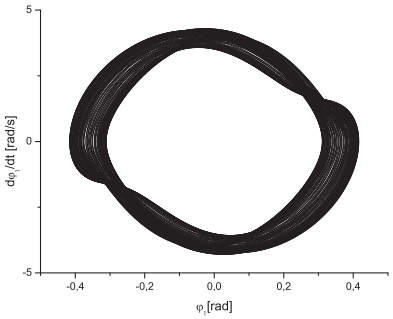

(c) Phase portrait $\omega_x = 9$ Hz

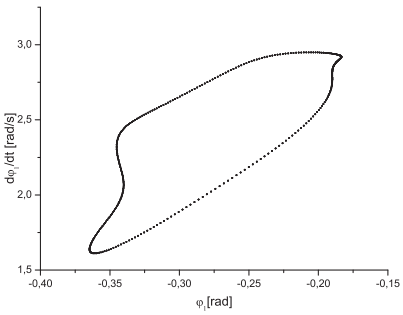

(d) Poincaré map ω_x =9 Hz

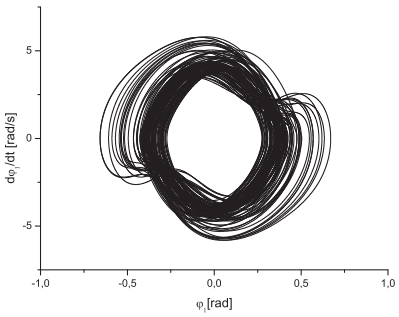

(e) Phase portrait $\omega_x = 9.2$ Hz

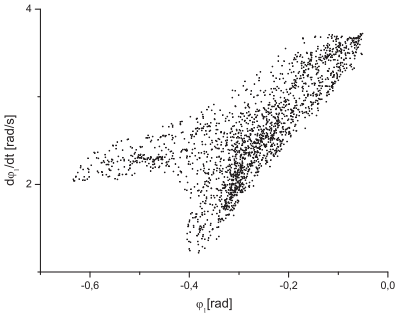

(f) Poincaré map $\omega_x = 9.2$ Hz

Figure 4.10: Phase portraits and Poincaré maps for $k_2 = 1000$ N/m

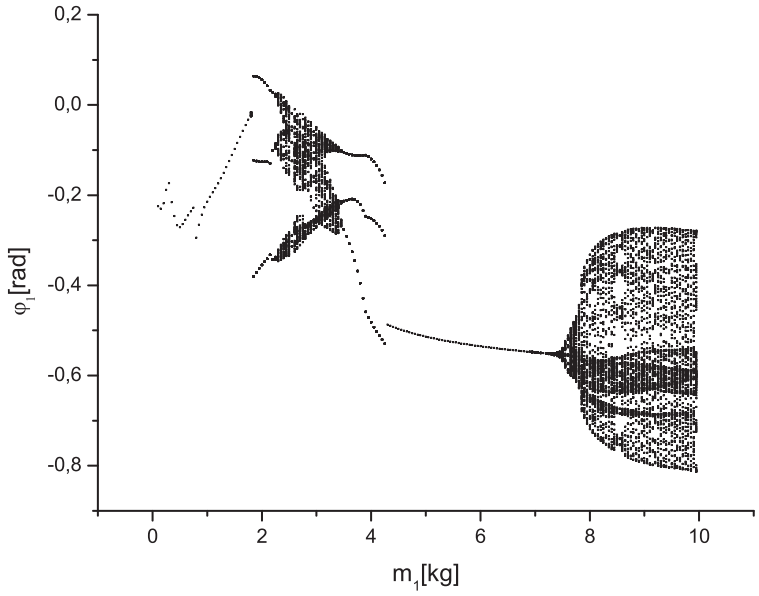

Figure 4.11: Forward bifurcation diagram for φ_1 with $k_2 = 500$ N/m and $\omega_x = 5.2$ Hz

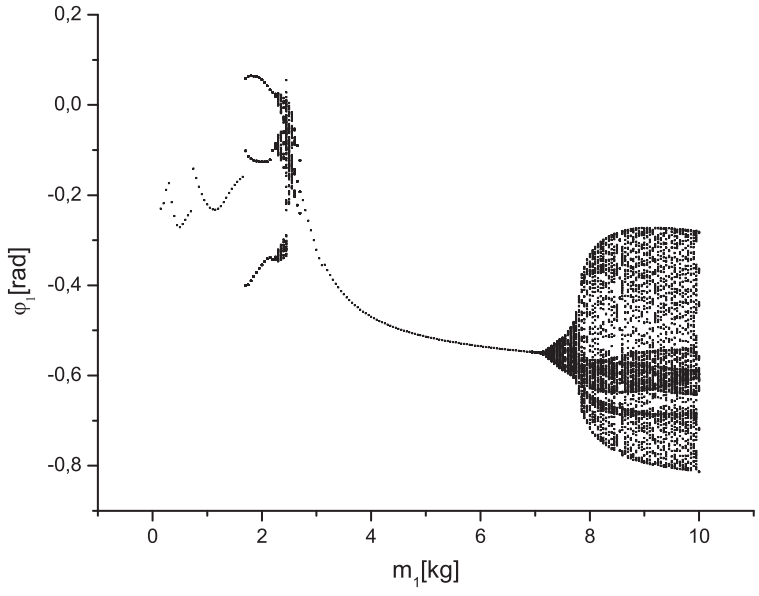

Figure 4.12: Backward bifurcation diagram for φ_1 with $k_2 = 500$ N/m and $\omega_x = 5.2$ Hz

The value of parameters selected for the bifurcation diagrams in Figures 4.11 and 4.12 were $\omega_x = 5.2$ Hz and $k_2 = 500$ N/m. To remind the results from Figures 4.1 and 4.2 for that value of ω_x and $m_1 = 2kg$, we deal with the attractor with period-3. The results in Figures 4.1 and 4.2 correspond to these in Figures 4.11 and 4.12. The phase diagrams and Poincaré map for selected values of m_1 2.45 kg, 7.5 kg and 9 kg (see Figure 4.13) indicate quasi-periodic behaviour. The periodic behaviour is detected for $3kg \leq m_1 \leq 7kg$, as well as for $m_1 < 2.3 \quad kg$.

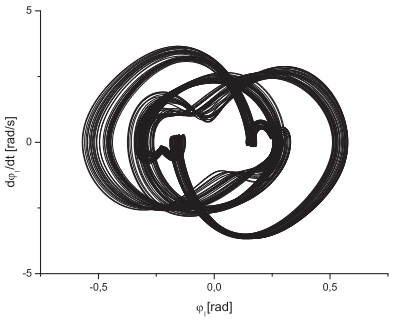

(a) Phase portrait $m_1 = 2.45$ kg

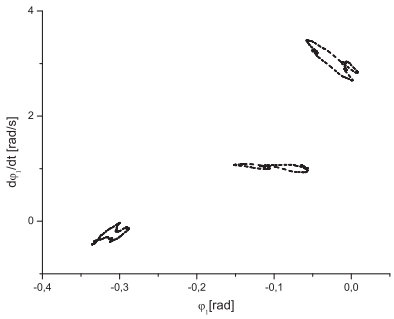

(b) Poincaré map $m_1 = 2.45$ kg

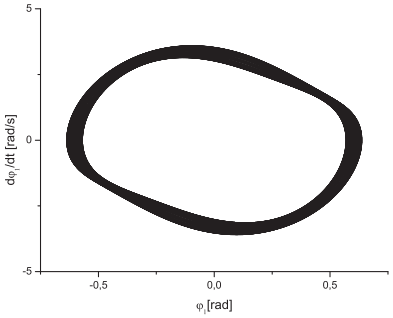

(c) Phase portrait $m_1 = 7.5$ kg

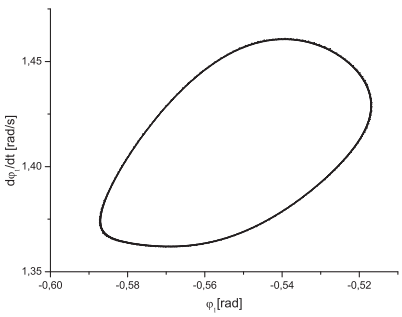

(d) Poincaré map $m_1 = 7.5$ kg

Figure 4.13: Phase portraits and Poincaré maps for $k_2 = 500$ N/m and $\omega_x = 5.2$ Hz

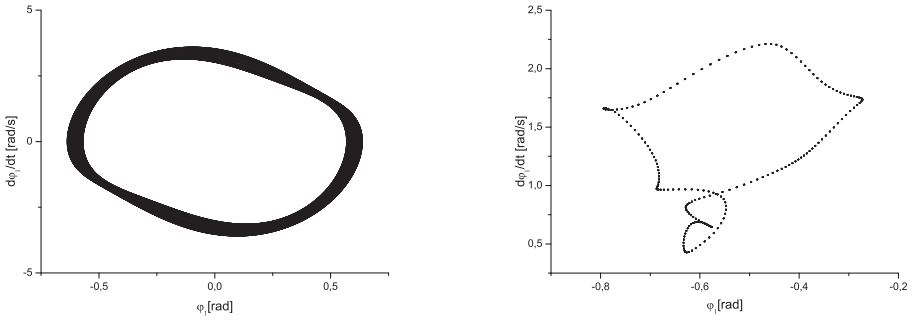

(a) Phase portrait $m_1 = 9$ kg (b) Poincaré map $m_1 = 9$ kg

Figure 4.14: Phase portraits and Poincaré maps for $k_2 = 500$ N/m and $\omega_x = 5.2$ Hz

Finally, the influence of mass m_1 on the system with spring constant $k_2 = 1000$ N/m and frequency of excitation $\omega_x = 8.4$ Hz was investigated. In Figures 4.7 and 4.8 for that particular frequency, a window of period-2 is observed. The bifurcation diagrams in Figures 4.15 and 4.16 reveal the routes to chaos by Hopf bifurcation ($m_1 = 2.45$ kg) and period doubling ($m_1 = 4$ kg). For the interval $m_1 \in [2.5, 4.6]$ a chaotic behaviour is observed. For m_1 the system has double period. These observations are also based on phase diagrams and Poincaré maps (see Figure 4.17).

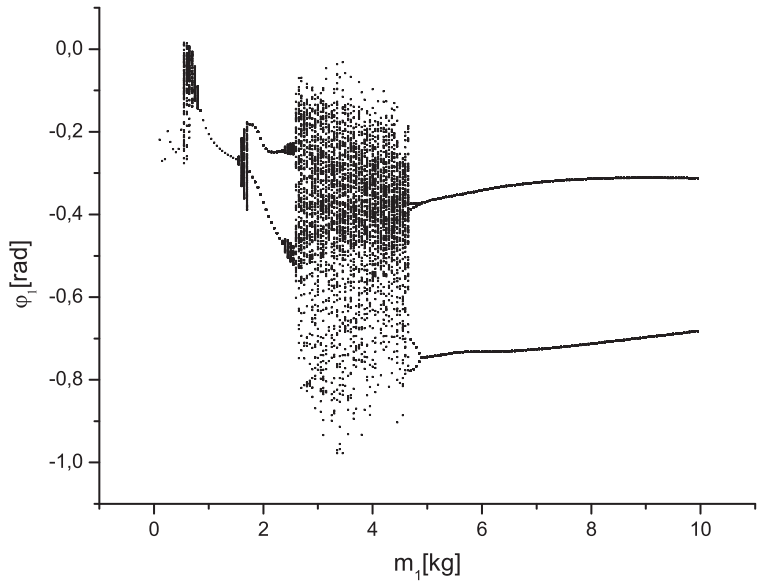

Figure 4.15: Forward bifurcation diagram for φ_1 with $k_2 = 1000$ N/m and $\omega_x = 8.4$ Hz

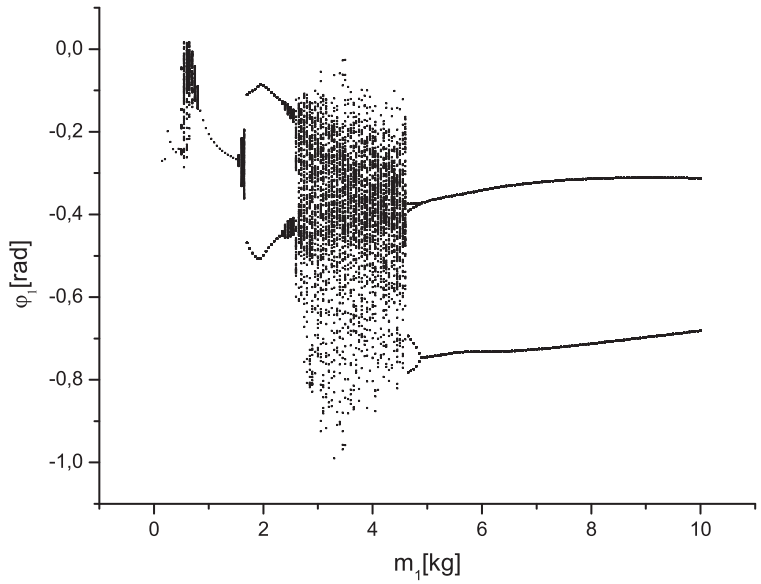

Figure 4.16: Backward bifurcation diagram for φ_1 with $k_2 = 1000$ N/m and $\omega_x = 8.4$ Hz

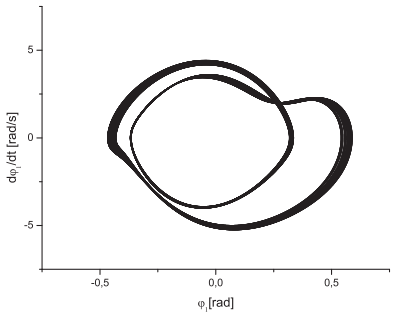

(a) Phase portrait $m_1 = 2.5$ kg

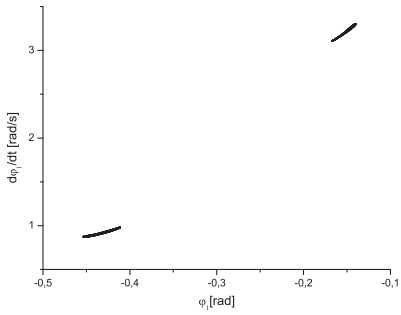

(b) Poincaré map $m_1 = 2.5$ kg

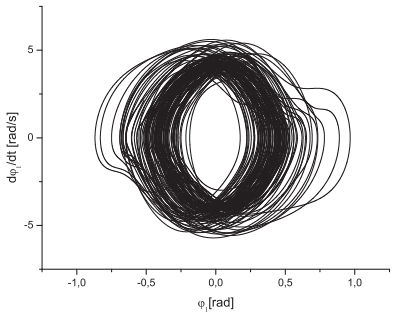

(c) Phase portrait $m_1 = 3.5$ kg

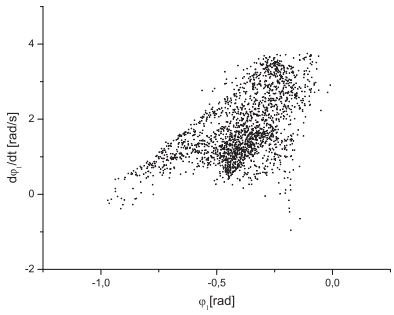

(d) Poincaré map $m_1 = 3.5$ kg

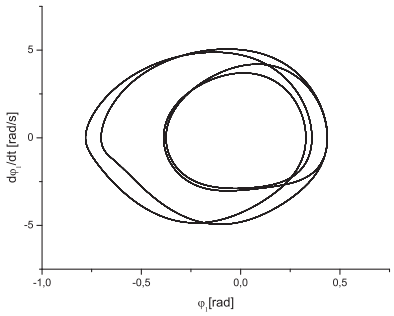

(e) Phase portrait $m_1 = 4.7$ kg

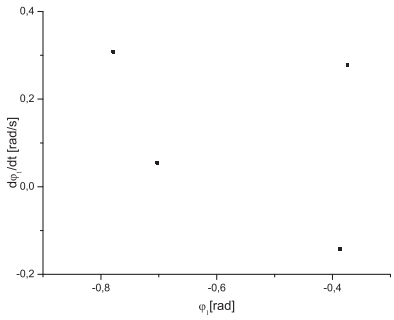

(f) Poincaré map $m_1 = 4.7$ kg

Figure 4.17: Phase portraits and Poincaré maps for $k_2 = 1000$ N/m and $\omega_x = 8.4$ Hz

Chapter 5

Conclusions

The investigated system was double pendulum with parametric horizontal excitation. The system has 3 degrees of freedom (two angles and length of the spring in the second limb). The testing methods involve bifurcation diagrams, phase diagrams and Poincaré maps. Numerical calculations were performed by means of the author's own program basing on GNU Scientific Library.

The most important case in the thesis was to check the influence of the excitation frequency on the system behaviour. During the analysis 3 types of behaviours were observed (i.e. periodic, quasi-periodic and chaotic). Generally, for both tested spring coefficients k_2 for most of the time the system remains periodic. For bigger values of excitation frequency ($\omega_x > 8$ Hz) the behaviour of the system changes. Either the numerical solution of the system changes the attractor or the system begins to behave quasi-periodically, eventually reaching chaos for $\omega_x \approx 10Hz$. The quasi-periodic regions prior to the chaotic ones indicate the sequence of Hopf bifurcation as route to chaos. Another observed route to chaos was period doubling which occur for bifurcations with mass m_1 as a bifurcation parameter.

Apart from investigating the influence of the excitation frequency,the relation between mass m_1 on the first limb of the pendulum for selected value of excitation frequency was calculated. The results led to detecting regions of periodic behaviour as well as quasi-periodic one.

For all bifurcation diagrams forward and backward bifurcation were performed which means that the bifurcation parameter was increased and after reaching the end of the investigated range decreased. The diagrams for forward and backward bifurcations behave similarly, however it is clearly visible that they follow slightly different attractors. It is an evidence of the co-existence of the solutions.

Bibliography

[1] F. Amirouche. *Fundamentals of Multibody Dynamics.* Birkhauser, Boston, 2006.

[2] V.I. Arnold. *Mathematical Methods of Classical Mechanics.* Springer, New York, 1989.

[3] R.H. Enns and G. McGuire. *Nonlinear physics with Maple for scientists and engineers.* Birkhauser, Boston, 2000.

[4] T. Kapitaniak. *Chaos for engineers.* Springer, New York, 1970.

[5] T. Kapitaniak. *Wstęp do teorii drgań.* Politechnika Łódzka, Łódź, 2005.

[6] T. Kapitaniak and J. Wojewoda. *Attractors of quasiperiodically forced systems.* World Scientific Publishing, Singapore, 1993.

[7] T. Kapitaniak and J. Wojewoda. *Bifurkacje i chaos.* Politechnika Łódzka, PWN, Warszawa - Łódź, 2000.

[8] M.R. Matthews, C.F. Gauld, and A. Stinner. *The Pendulum: Scientific, Historical, Philosophical and Educational Perspectives.* Springer, Dordrecht, 2005.

[9] W. Rubinowicz and W. Królikowski. *Mechanika Teoretyczna.* PWN, Warszawa, 1998.